Available online at www.sciencedirect.com
SCIENCE DIRECT®
Journal of Power Sources 142 (2005) 125–133
JOURNAL OF POWER SOURCES
www.elsevier.com/locate/jpowsour

Effects of baffle-blocked flow channel on reactant transport and cell performance of a proton exchange membrane fuel cell

Hui-Chung Liu[a], Wei-Mon Yan[a,*], Chyi-Yeou Soong[b], Falin Chen[c]

[a] *Department of Mechatronic Engineering, Huafan University, Shih Ting, Taipei 223, Taiwan, ROC*
[b] *Department of Aerospace and System Engineering, Feng Chia University, Seatwen, Taichung 40724, Taiwan, ROC*
[c] *Institute of Applied Mechanics, National Taiwan University, Taipei 106, Taiwan, ROC*

Received 26 August 2004; accepted 16 September 2004
Available online 15 December 2004

Abstract

The objective of the present study is to investigate the application of the baffle-blocked flow channels for enhancement of reactant transport and cell performance of a proton exchange membrane fuel cell (PEMFC). It is expected that due to the blockage effects in the presence of the baffles, more fuel gas in the flow channel can be forced into the gas diffuser layer to enhance the chemical reactions and then augment the performance of the PEMFC systems. The effects of liquid water formation on the reactant gas transport are taken into account in the present modeling. Predictions show that the local transport of the reactant gas, local current density generation, and the cell performance can be enhanced by the presence of the baffles. A physical interpretation for the difference in the baffle effects at high and low operating voltages is presented. The results reveal that, at low voltage conditions, the liquid water effect is especially significant and should be considered in the modeling. The cell performance can be enhanced at a higher air velocity on the cathode side, by which the cell performance can be enhanced and occurrence of the mass transport loss can be delayed with the limiting current density raised considerably.
© 2004 Elsevier B.V. All rights reserved.

Keywords: Proton exchange membrane fuel cell; Reactant transport; Baffles

1. Introduction

Fuel cell is an electro-chemical system that can realize the direct conversion of chemical energy of reactants (a fuel with an oxidant) to electric energy with high efficiency and high environment compatibility. A proton exchange membrane fuel cell (PEMFC) operates at significantly low temperature than other types of fuel cells do. It is a potential candidate of the power source in the near future. There exist a number of studies on the transport phenomena and the performance of the PEM fuel cells in the open literature. Springer et al. [1] proposed an isothermal, one-dimensional model for the proton exchange membrane fuel cells. In their model, water diffusion coefficient, electro-osmotic drag coefficient, water sorption isotherms, and the membrane conductivities were assumed to be functions of membrane water content. Results showed that the membrane resistance can be significantly raised with an increase in current density, and the net water flux ratio under typical condition is much less than that under the fully hydrated membrane. It was also found that the resistance then reduces for a membrane of thickness small enough. Kim et al. [2] presented an empirical equation to fit the experimental data of cell potential and current density for the PEM fuel cells at various operating conditions of temperatures, pressures, and oxygen compositions in the cathode gas mixture. Singh et al. [3] employed a two-dimensional model to investigate the transport phenomena in a PEMFC. In their work, the attention was focused on the transport processes in fuel cells in order to improve the thermal and water management, and to alleviate the mass transport limitations. To examine the effects of temperature and gas pressure gradients on fuel cell performance and water management, a one-dimensional, non-isothermal model was proposed by Djilali

* Corresponding author. Tel.: +886 2 2663 2102; fax: +886 2 2663 1119.
E-mail address: wmyan@huafan.hfu.edu.tw (W.-M. Yan).

0378-7753/$ – see front matter © 2004 Elsevier B.V. All rights reserved.
doi:10.1016/j.jpowsour.2004.09.037

Nomenclature

C	mass fraction
C_F	quadratic drag factor
D	mass diffusivity ($m^2\ s^{-1}$)
F	Faraday constant (96,487 C mol^{-1})
I	current density ($A\ m^{-2}$)
J	transfer current density ($A\ m^{-2}$)
k_p	permeability
l_c	gas channel length (m)
l_g	gap between diffuser layer and baffle (m)
N	number of baffles
P	pressure (Pa)
R	universal gas constant (8.314 J $(mol\ K)^{-1}$)
S	molar production rate per unit area
T	temperature (K)
u	velocity in the x-direction ($m\ s^{-1}$)
v	velocity in the y-direction ($m\ s^{-1}$)
V	operating voltage (V)
w	oxygen mass fraction
Z_f	Spices valence

Greek symbols

α	transfer coefficient for the reaction
ε	porosity
η	surface overpotential (V)
λ	channel width fraction, l_g/l_c
ρ	density of oxygen ($kg\ m^{-3}$)
σ	ionic conductivity of the ionomer ($\Omega^{-1}\ m^{-1}$)
τ	tortuosity of diffusion layer
Φ	phase potential
υ	viscosity of flow
ϕ	ionomer phase potential (V)

Subscripts

a	anode
c	cathode
m	membrane
d	diffuser layer
u	x-direct
v	y-direct
L	liquid water
eff	effective

and Lu [4]. It was found that the temperature distribution in the PEMFC is affected by the water phase change in the electrode. The peak temperature within the cell occurs at lower operating temperature and partially humidified reactants. As a result of enhanced water evaporation with thermal gradients taken into account, the Darcy isothermal pressure drop can be compensated by the temperature non-uniformity.

In the study of the PEM fuel cells, the thermal and water management is one of the most important issues. Nguyen and White [5] proposed a model of the water and heat management of the PEMFC systems, which includes the effect of electro-osmosis, diffusion of water, heat transfer from solid phase to gas phase, and latent heat as water evaporation and condensation. They found that the ohmic loss is considerable at high current density and the voltage loss is twice amount of that of the cathode electrode. The back-diffusion of the water from the cathode to the anode is not enough to keep the membrane hydrated. Therefore, the reactant gas at the anode needs to be humidified. In their work, Voss et al. [6] developed a relatively novel technique of water management with anode water removal to modify the water concentration profile or gradient of the proton exchange membrane to augment the back-diffusion rate of water from the cathode to the anode. Therefore, the water at the cathode catalyst layer diffuses through the membrane and is removed via the anode reactant gas stream. Yi and Nguyen [7] proposed an along the channel model for evaluating the effects of various design and operating parameters on the performance of a PEMFC. The results show that humidification of the anode gas is required to enhance the conductivity of the membrane, and the liquid injection and higher humidification temperature can improve the cell performance by introducing more water into the anode. Also applying higher cathode gas pressure helps to replenish the water loss by electro-osmosis, thereby making the membrane more conductive and thus resulting in higher cell performance. Baschuk and Li [8] developed a mathematical model with variable degrees of water flooding in the PEMFC. Physical and electrochemical processes occurring in the membrane electrolyte, the cathode catalyst layer, the electrode backing layer and the flow channel were considered. Compared with experimental results, they found that when air was used as the cathode fuel, the flooding phenomena are similar at different operating conditions of the pressures and temperatures. When cell pressure is increased significantly, the water flooding in the electrode becomes serious and leads to a noticeable reduction in the power output.

The design of the flow field in bi-polar plate is one of the crucial factors to the performance of a PEMFC. To enhance the liquid water transport out of the diffuser layer, a new flow channel design was developed by Nguyen [9]. This design in effect has converted the transport of reactant/product gases to/from the catalyst layers from diffusion mechanism to a convection mechanism. Wood et al. [10] presented the experimental results on the effectiveness of the direct liquid water injection scheme and interdigitated flow field design for proving the performance of PEMFCs. They found that the interdigitated flow field is able to provide higher transport rates of reactant and products to and from the inner catalyst layers. To understand the effects of the interdigitated gas distributor on the performance of these fuel cell electrodes, Yi and Nguyen [11] proposed a two-dimensional isothermal model of a porous electrode to simulate the hydrodynamics of gas flow through the pore volume of the electrode of a PEMFC. Based on the predicted results, it was concluded

that the electrode performance is improved by the higher gas flow rate through the electrode improves. Besides, the average current density decreases with an increase in the electrode thickness or shoulder width of the gas distributor.

He et al. [12] studied the effects of various electrode and flow field design parameters on the performance of the cathode of a PEMFC. It was found that that higher differential pressure between inlet and outlet channels will enhance the electrode performance. Increasing the electrode thickness is equivalent to increasing the diameter of a pipe in a fluid flow system and the gas bypassing effect becomes more significant. Um and Wang [13,14] developed a multidimensional model to study the electrochemical kinetics, current distribution, fuel and oxidant flow, and multicomponent transport in a PEMFC with the interdigitated flow field. The electrochemical behaviors of a direct methanol fuel cell with serpentine flow field (SFF) and interdigitated flow field (IFF) at both cathode and anode were investigated by Arico et al. [15]. The experimental results showed that the IFFs significantly enhance the mass transport inside a DMFC and allow achieving the higher maximum power outputs compared to the classical serpentine geometry. The larger methanol permeation through the electrolyte determines both lower voltage and fuel efficiencies in the activation-controlled region with respect to the SFF. Recently, Yan et al. [16,17] presented the studies about the effects of flow channel designs on the steady or dynamic gas transport and cell performance of PEM fuel cells. They found that the flow distributor geometry has a significant influence on the cell performance. In addition, they indicated that for a larger channel width fraction, a faster dynamic response as well as better cell performance can be attained.

With the appropriate design of the flow channel of the bipolar plate, the efficiency of the thermal and water management in PEMFC systems can be achieved. Therefore how to design an optimal flow channel in the bipolar plate is one of the most important issues in the study of the PEMFC. To install a tandem array of baffles in fuel flow channels is a possible strategy. It is expected that due to the blockage effects in the presence of the baffles, more fuel gas in the flow channel can be forced into the gas diffuser layer to enhance the chemical reactions and, in turn, augment the performance of the PEMFC systems. From the literatures reviewed above, it is obvious that the performance of the blocked flow channels with baffles installed in a PEMFC have not been well examined yet. This motivates the present study. The objective of the present study is to investigate the performance of the blocked flow channel with baffles in a proton exchange membrane fuel cells (PEMFC) is investigated numerically. A two-dimensional numerical model is developed to carry out the reactant gas transport phenomena and cell performance with baffle effects in the flow channel of bipolar plate. Effects of the baffle width are explored. Additionally, the effects of liquid water formation on the reactant gas transport are taken into account in the modeling and examined in the analysis.

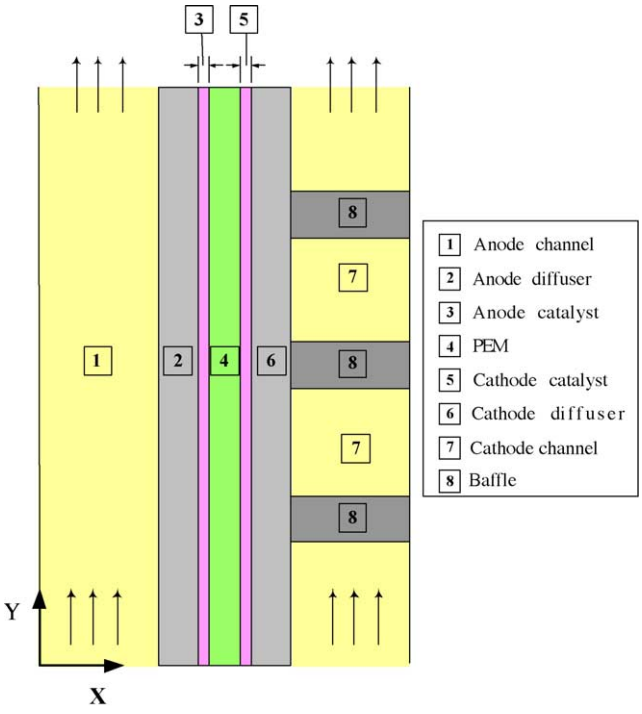

Fig. 1. Two-dimensional fuel cell model of a PEMFC system with baffle-blocked flow channel.

2. Analysis

Fig. 1 is a schematic diagram of the two-dimensional fuel cell model of the PEMFC considered in the present work, which consists of a proton exchange membrane, two catalyst layers, two gas diffuser layers, and two flow channels. To examine the effects of the baffles on the gas transport and cell performance, the tandem array of the baffles is arranged in the cathode flow channel in order to force the fuel gas to flow into the gas diffuser layer and catalyst layer at the cathode side. For simplification of the analysis, the following assumptions are invoked: (1) the gas mixtures are considered to be perfect gases; (2) the gas flow is steady and laminar everywhere in the fuel cell; (3) the gas diffuser layers, catalyst layers, and the PEM are considered to be isotropic porous media; (4) the heat generated by the chemical reaction is neglected in this work.

With the above assumptions, the gas transport equations for a two-dimensional PEMFC system can be depicted as follows.

Continuity equation :
$$\frac{\partial u}{\partial x} + \frac{\partial v}{\partial y} = 0 \tag{1}$$

Momentum equations:

$$\varepsilon_{\text{eff}} \left(u\frac{\partial u}{\partial x} + v\frac{\partial u}{\partial y} \right) = -\frac{\varepsilon_{\text{eff}}}{\rho}\frac{\partial P}{\partial x} + \upsilon\varepsilon_{\text{eff}} \left(\frac{\partial^2 u}{\partial x^2} + \frac{\partial^2 u}{\partial y^2} \right) + S_u \tag{2}$$

Table 1a
Parameters used in this work

Porosity of diffuser layer	0.4
Porosity of catalyst layer	0.4
Baffle width (m)	0.000762
Channel length (m)	0.0762
Channel width (m)	0.000762
Diffuser layer width (m)	0.000254
Catalyst layer width (m)	0.0000287
Membrane width (m)	0.00023
Operation temperature (K)	353
Operation pressure (atm)	1
Inlet average velocity, v_0 (m s^{-1})	1.76

$$\varepsilon_{\text{eff}}\left(u\frac{\partial v}{\partial x}+v\frac{\partial v}{\partial y}\right)=-\frac{\varepsilon_{\text{eff}}}{\rho}\frac{\partial P}{\partial y}+\upsilon\varepsilon_{\text{eff}}\left(\frac{\partial^2 v}{\partial x^2}+\frac{\partial^2 v}{\partial y^2}\right)+S_v \tag{3}$$

$$\text{Species concentration equation}: \quad \varepsilon_{\text{eff}}\left(u\frac{\partial C_k}{\partial x}+v\frac{\partial C_k}{\partial y}\right)=D_{k,\text{eff}}\left(\frac{\partial^2 C_k}{\partial x^2}+\frac{\partial^2 C_k}{\partial y^2}\right)+S_k+S_{\text{L}} \tag{4}$$

In the momentum equations, S_u and S_v stand for the source terms based on the Darcy's drag forces in the x and y directions imposed by the pore walls on the fluid, and usually cause in a significant pressure drop across the porous media. The details of S_u and S_v for different layers are listed in Tables 1a and 1b.

In Eq. (4), the effective mass diffusivity, D_{eff}, can be written as $D_{k,\text{eff}}=D_k\varepsilon^{\tau_i}$ and τ_i is the tortuosity of the pores in porous medium and S_k is the production rates of kth species in gas phase.

To comprehend the liquid water effect, a simplified two-phase model is used to describe water transport in the PEM fuel cell. In this work, we account for the liquid water effect by modify the mass diffusivity due to the liquid water filling the pores in the porous media and the liquid water generation in the species concentration equation. When the partial pressure of water vapor is greater than the saturation pressure of water vapor, we assume that water vapor may condense and fill the pore in the porous media. The source term, S_{L} in the species concentration equation, Eq. (4), representing the quality of liquid water can be evaluated [18]:

$$S_{\text{L}}=\begin{cases}M_{\text{H}_2\text{O}}k_{\text{c}}\frac{\varepsilon_{\text{eff}}C_{\text{H}_2\text{O}}}{\rho RT}(P_{\text{H}_2\text{O}}-P_{\text{sat}}), & \text{if } P_{\text{H}_2\text{O}}>P_{\text{sat}}\\ k_{\text{e}}\varepsilon_{\text{eff}}s(P_{\text{sat}}-P_{\text{H}_2\text{O}}), & \text{if } P_{\text{H}_2\text{O}}<P_{\text{sat}}\end{cases} \tag{5}$$

where M is the molecular weight and k_{c} and k_{e} are the condensation and evaporation rate constants, respectively. The saturation pressure of water can be expressed as

$$P_{\text{sat}}=10^{-2.1794+0.02953T-9.1837\times10^{-5}T^2+1.4454\times10^{-7}} \tag{6}$$

In addition, the saturated rate, s, is defined as the ratio of the volume of pore occupied by liquid water to the volume of pore in the porous medium.

For this reason, the effective porosity of porous media is modified to account the liquid water effect:

$$\varepsilon_{\text{eff}}=\varepsilon(1-s) \tag{7}$$

The phase potentials in the catalyst layers satisfy the following equations:

$$\frac{\partial}{\partial x}\left(\sigma_{\text{m}}\frac{\partial \Phi}{\partial x}\right)+\frac{\partial}{\partial y}\left(\sigma_{\text{m}}\frac{\partial \Phi}{\partial y}\right)=-j_{\text{a}} \quad \text{at anode} \tag{8}$$

$$\frac{\partial}{\partial x}\left(\sigma_{\text{m}}\frac{\partial \Phi}{\partial x}\right)+\frac{\partial}{\partial y}\left(\sigma_{\text{m}}\frac{\partial \Phi}{\partial y}\right)=-j_{\text{c}} \quad \text{at cathode} \tag{9}$$

and the phase current density satisfies as following equations:

$$\frac{\partial i_x}{\partial x}+\frac{\partial i_y}{\partial y}=j_{\text{a}} \quad \text{at anode} \tag{10}$$

$$\frac{\partial i_x}{\partial x}+\frac{\partial i_y}{\partial y}=j_{\text{c}} \quad \text{at cathode} \tag{11}$$

The governing equation of the proton concentration in the membrane can be written as

$$\varepsilon_{\text{m}}\left(u\frac{\partial C_k}{\partial x}+v\frac{\partial C_k}{\partial y}\right)=D_{i,\text{eff}}\left(\frac{\partial^2 C_k}{\partial x^2}+\frac{\partial^2 C_k}{\partial y^2}\right)+\frac{ZF}{RT}D_{i,\text{eff},\text{H}^+}W_{\text{H}^+}\left(\frac{\partial^2 \Phi}{\partial x^2}+\frac{\partial^2 \Phi}{\partial y^2}\right) \tag{12}$$

Table 1b
Details of the source terms in the governing equations

	S_u	S_v	S_k	$D_{k,\text{eff}}$	τ_i
Gas channel	0	0	0	–	–
Gas diffuser layers	$-\frac{\upsilon\varepsilon^2}{k_{\text{p}}}u-\frac{\varepsilon^3 C_{\text{F}}\rho u}{\sqrt{k_{\text{p}}}}\sqrt{u^2+v^2}$	$-\frac{\upsilon\varepsilon^2}{k_{\text{p}}}v-\frac{\varepsilon^3 C_{\text{F}}\rho v}{\sqrt{k_{\text{p}}}}\sqrt{u^2+v^2}$	0	$D_k\varepsilon_{\text{d,eff}}^{\tau_i}$	1.5
Catalyst layers	$-\frac{\upsilon\varepsilon^2}{k_{\text{p}}}u-\frac{\varepsilon_{\text{eff}}^3 C_{\text{F}}\rho u}{\sqrt{k_{\text{p}}}}\sqrt{u^2+v^2}$	$-\frac{\upsilon\varepsilon^2}{k_{\text{p}}}v-\frac{\varepsilon_{\text{c,eff}}^3 C_{\text{F}}\rho v}{\sqrt{k_{\text{p}}}}\sqrt{u^2+v^2}$	H_2: $-\frac{1}{2FC_{\text{a}}}j_{\text{a}}$ O_2: $-\frac{1}{4FC_{\text{c}}}j_{\text{c}}$ H_2O: $\frac{1}{2FC_{\text{c}}}j_{\text{c}}$	$D_k\varepsilon_{\text{c,eff}}^{\tau_i}$	1.5
Membrane	$-\frac{\upsilon\varepsilon^2}{k_{\text{p}}}u-\frac{\varepsilon_{\text{eff}}^3 C_{\text{F}}\rho u}{\sqrt{k_{\text{p}}}}\sqrt{u^2+v^2}+\frac{k_{\text{p}}}{\nu}Z_{\text{f}}C_{\text{H}^+}F\cdot\nabla\Phi\cdot\frac{\partial u}{\partial x}$	$-\frac{\upsilon\varepsilon^2}{k_{\text{p}}}v-\frac{\varepsilon_{\text{eff}}^3 C_{\text{F}}\rho v}{\sqrt{k_{\text{p}}}}\sqrt{u^2+v^2}+\frac{k_{\text{p}}}{\nu}Z_{\text{f}}C_{\text{H}^+}F\cdot\nabla\Phi\cdot\frac{\partial v}{\partial x}$	$\frac{ZF}{RT}D_{k,\text{eff},\text{H}^+}C_{\text{H}^+}\left(\frac{\partial^2\Phi}{\partial x^2}+\frac{\partial^2\Phi}{\partial y^2}\right)$	$D_k\varepsilon_{\text{m,eff}}^{\tau_i}$	6

and the membrane phase potential is governed by the following equation:

$$\frac{\partial}{\partial x}\left(\sigma_{\mathrm{m}}\frac{\partial \Phi}{\partial x}\right)+\frac{\partial}{\partial y}\left(\sigma_{\mathrm{m}}\frac{\partial \Phi}{\partial y}\right)=0 \tag{13}$$

In the above formulations, Eqs. (1)–(4) and (8)–(13) form a complete set of governing equations. The detailed boundary conditions are similar to those of Soong et al. [19]. Due to the space limit, they are not presented here.

3. Numerical method

Since it is impossible to obtain an analytic solution of the complex convection–diffusion problem like this one, it will be solved by a finite volume method using a collocated cell-centered variable arrangement. The governing equations can be expressed in the form of a generalized transport equation

$$\nabla\cdot(\rho\vec{u}\phi-\Gamma_{\phi}\nabla\phi)=S_{\phi} \tag{14}$$

where ϕ is the general dependent variable, Γ_{ϕ} the exchange coefficient, S_{ϕ} the source term, $\vec{u}$ velocity vector, and ρ the density. With the discretization of the governing equations, the coupled finite-difference equations become

$$a_{\mathrm{P}}\phi_{\mathrm{P}}=a_{\mathrm{E}}\phi_{\mathrm{E}}+a_{\mathrm{W}}\phi_{\mathrm{W}}+a_{\mathrm{N}}\phi_{\mathrm{N}}+a_{\mathrm{S}}\phi_{\mathrm{S}}+S_{\phi} \tag{15}$$

where ϕ_{P} is the value of ϕ at the current point P, $\phi_{\mathrm{E}}\ldots\phi_{\mathrm{S}}$ stand for the values of the grid points adjacent to the point P, and $a_{\mathrm{P}}\ldots a_{\mathrm{S}}$ are known as the link coefficients.

In this work, the non-uniformly distributed grid systems of 101 and 183 points are employed in the x and y directions (or expressed as 101×183), respectively. To obtain better accuracy in the numerical computations, grid independence is examined in the preliminary test runs. It is found that the deviations of the local current density between the predictions on the grids of 101×183 and 201×285 are less than 2%. According, the computations on the grid system of 101×183 points seems sufficient to understand the behaviors of the reactant gas transport in a PEMFC. To further check the adequacy of the numerical scheme, at first, the results of the two-dimensional results without the baffle effect are evaluated, as shown in Fig. 2. It is clearly seen from Fig. 2 that the present predictions agree reasonably with the experimental data of Chen [20]. The above preliminary runs confirm that the present model and the numerical method used are generally appropriate in analysis of the present problem.

4. Results and discussion

With the tandem arrangement of the baffles in the channel of the cathode side, the fuel gas will be forced to flow into the gas diffuser layer and catalyst layer to enhance the chance of chemical reaction at the catalyst layer as well as the performance of the fuel cell system. To examine the baffle

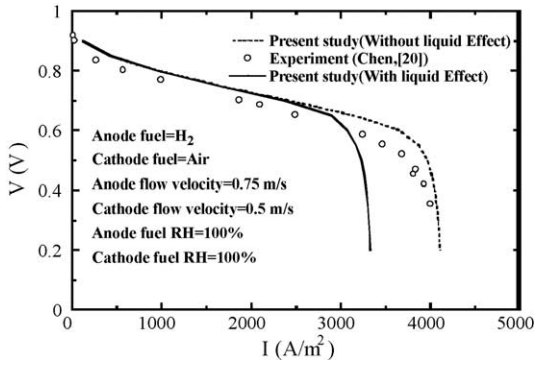

Fig. 2. Comparison of the predicted *I–V* curve without baffle effect and the experimental data of Chen [20].

effects on the cell performance, the polarization (*I–V*) curves with various baffle width and baffle numbers are presented in Fig. 3(a) and (b), respectively. For comparison, the results without liquid water effects in the model are also presented. An overall inspection of Fig. 3 indicates that at the conditions of the high operating voltages, the baffle effects on the overall cell performance are negligibly small as compared with those without baffle effect. At low voltage conditions, however, the baffle effects on the *I–V* curves become important. In addition, the cell performance is enhanced with increase in the

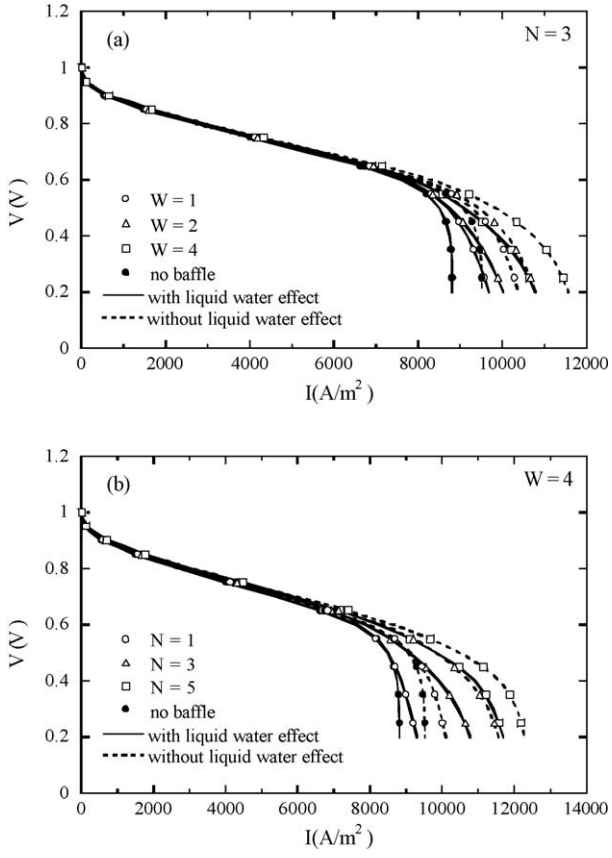

Fig. 3. Effects of baffle width and baffle numbers on the cell performance: (a) baffle width effects and (b) baffle number effects.

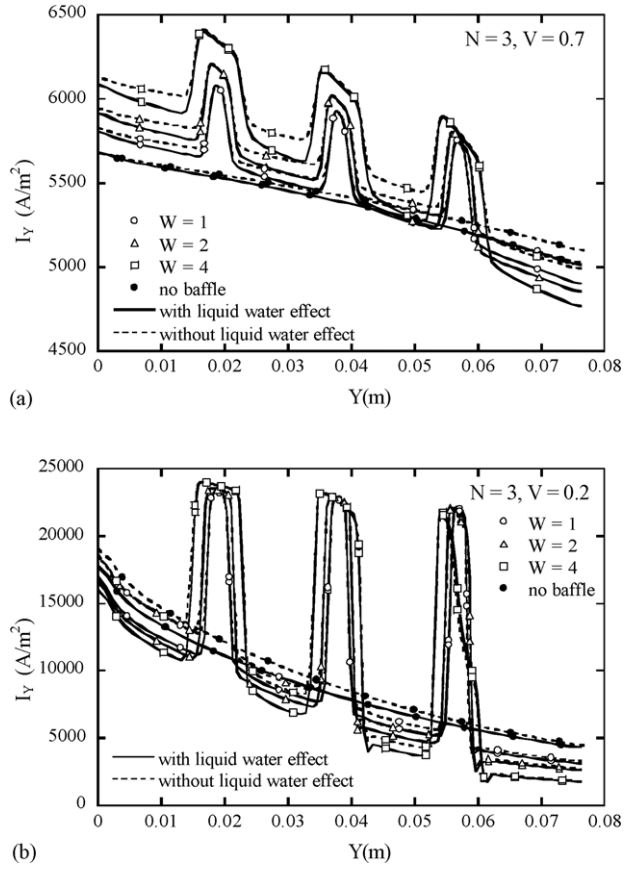

Fig. 4. Effects of baffle width on the local current density distributions: (a) $V = 0.7$ V and (b) $V = 0.2$ V.

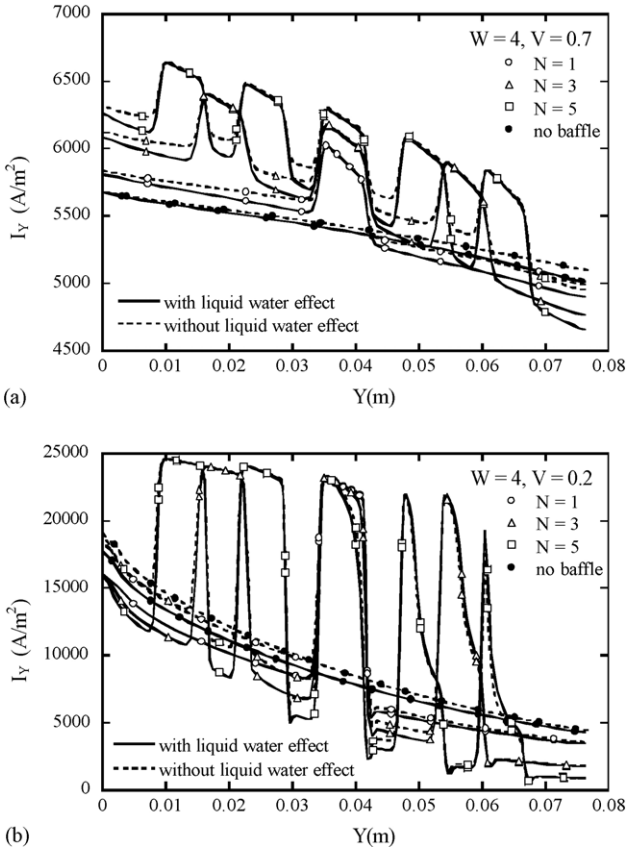

Fig. 5. Effects of baffle number on the local current density distributions: (a) $V = 0.7$ V and (b) $V = 0.2$ V.

baffle width and/or baffle numbers. It is clearly seen that the higher limiting current density is noted for a PEMFC with a greater baffle width and/or baffle numbers. It is also disclosed that, at high operating voltage conditions, the deviations in the cell performance between the results with and without consideration of liquid water effects are small. This means that the fuel transport in the PEMFC can be safely treated as gas phase only at a high voltage condition. Whereas, at low voltage conditions, the liquid water effects on the cell performance are remarkable and cannot be neglected in the modeling. This confirms the fact that the mass transports at low V are significant and, in turn, more water is generated in the catalyst layer of the cathode side. Therefore, two-phase flow effects should be considered in the low operating voltage conditions.

The above evidences demonstrated that the appearance of the baffles in the flow channel has a considerable impact on the cell performance. It is very significant to examine the baffle effects on the local transport characteristics of the PEMFC, especially at the operating conditions of low voltage. To reach this end, Figs. 4 and 5 show the effects of baffle width and baffle numbers on the local current density distributions, respectively. In these plots, the baffles are located at the positions of $i/(N + 1)$th length from the cathode inlet. For example, for case of one baffle (i.e., $N = 1$), the baffle location is on the location of the 1/2th length from the inlet, that is, at the central position of the channel length. For $N = 3$, the three baffles are located at the positions of 1/4, 1/2 and 3/4th length from the inlet, respectively. It is clearly observed from Fig. 4 that except the peak regions, the local current density decreases with the axial location Y. However, around the baffle locations, there exist peaks in the distributions of the local current density. It means that better cell performance is generated around the baffle locations. This can be made plausible by noting the fact that as the fuel gas is blocked by the baffle in the channel, more fuel gas will be forced to turn into and penetrate through the gas diffuser layer and catalyst layer, which in turn, causes a significant enhancement of chemical reaction at the catalyst interface. The plots show local current density distributions of a periodic pattern with peak value appearing in the regions around the baffles and reducing along the channel. The best enhancement does always occur at the region around the first baffle. A careful examination of the cases with $V = 0.7$ V in Fig. 4(a) discloses that, the local current density monotonically increases with an increase in the baffle width in the upstream region quite near the entrance; while, at the downstream region ($Y > 0.065$ m) of the blocked channel with wider baffles, remarkable reductions in current density are found and the reduction becomes more serious as the baffle number N increases. The dramatic degradation in

local current density in the downstream region of a blocked channel is a reflection of the more efficient fuel transport and the chemical reaction in the upstream. Consequently, these two counter-effects render the resultant current density or performance of the fuel cell insensitive to the application of the baffles. For the cases with $V = 0.2$ V in Fig. 4(b), abrupt increases in current density appear due to the presence of the baffles, and the high-I regions beneath the baffles expend with an increase in the baffle width. Although the values of the current density in the regions between the neighboring baffles reduce with the increasing baffle width, in sum, noticeable enhancement in the cell performance can be still retained. The global effects addressed above for the cases with the baffles of various width at the operating conditions of 0.7 and 0.2 V can be validated in the I–V curves in Fig. 3(a). Besides, the predictions reveal that consideration of the liquid water in the simulation leads to the relatively lower current density than those in the cases without liquid water effect.

Fig. 5 presents the effects of baffle numbers on the local current density distributions for the baffle width $W = 4$ and at the operating voltages of 0.7 and 0.2 V. Generally, the qualitative trend of the data in Fig. 5 can be interpreted in a similar way as that we did for the cases of various baffle width effects in Fig. 4. The major difference between two is that the enhancement in local current density in Fig. 4 is achieved by enlarging the extend of the high-I regions via an increase in the baffle width, whereas in the cases shown in Fig. 5, the local current density or performance is enhanced by increasing the number of the high-I regions. The effects of the baffle number effects at the operating condition of low voltage ($V = 0.2$ V) are shown in Fig. 5(a). Near the entrance, the effects of baffle on the local current density are similar to those at the high operating voltage. For the downstream region, however, the peak-value regions in the local current density plots become narrow and shortened. This can be attributed to the more pronounced electro-chemical reaction at the operating condition of low voltage. Therefore, oxygen concentration at the cathode side would be reduced considerably, especially for the cases with a greater number of baffles. Accordingly, in the downstream region of the blocked channels, the high-I region around the baffle becomes narrow.

The distributions of oxygen mass flow rate along the interface between the gas diffuser layer (GDL) and catalyst layer (CL) with various arrangements of the baffles are presented in Fig. 6. Since the power output is the consequence of the electro-chemical reaction, the consumption of the oxygen along the GDL–CL interface can be considered as an index of the cell performance. A higher mass flow rate indicates a higher current density, i.e., a better cell performance. It is apparent that the distributions of the oxygen mass flow rate are similar to those of the local current density. This confirms the adequacy of the present study.

In the study of reactant gas transport in the PEMFC, understanding of the detailed local distributions of the oxygen at the cathode side along the GDL–CL interface is important to the design of a PEMFC. To this end, the effects of baffle

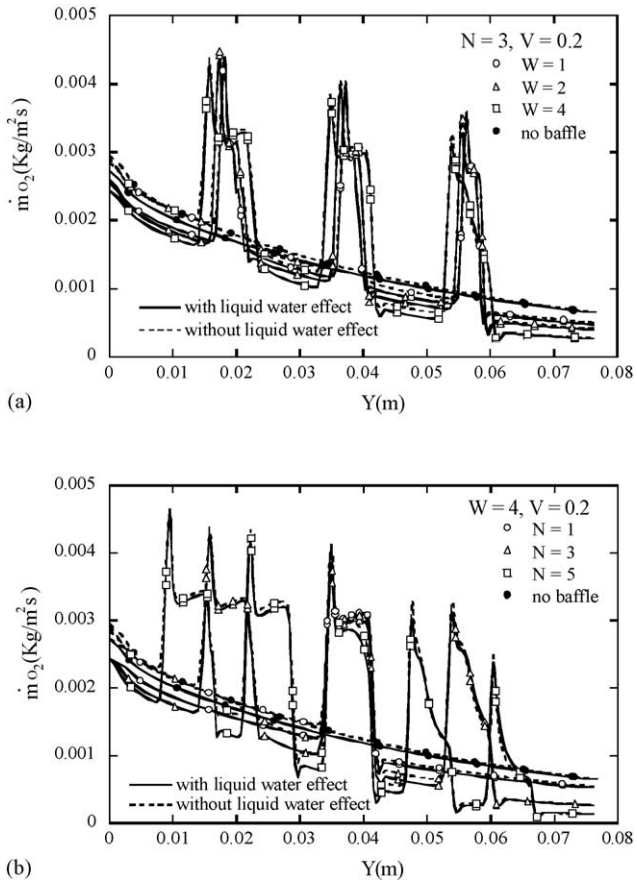

Fig. 6. Effects of baffle width and baffle number on the local distributions of oxygen mass flow rate.

width and baffle numbers on the local distributions of oxygen mass fraction along the GDL–CL interface for $V = 0.2$ V are presented in Fig. 7, in which it is observed that the presence of the baffles in the flow channel has a considerable impact on the local distributions of oxygen. Around the baffle regions, the oxygen distributions show a peaked increase, which is a consequence of the channel blockage and its effect on the enhancement of fuel gas transport we have addressed previously. Therefore, the oxygen distributions show peaked variations around the baffles. In Fig. 7(a), for the peaked variation around the first baffle, the influenced regions due to the presence of the baffle increases with the increased baffle width. But for the third peaked variation, the smallest influenced region and peak value in the oxygen concentration are noted in the case with a widest baffle, in which the chemical reaction along the catalyst in stronger near the entrance. But as the fuel gas goes downstream, the oxygen concentration becomes lower due to the faster consumption. Therefore, in the downstream region, the oxygen concentration may become lower around the baffle for the case with a wider baffle. As to the baffle numbers effects on the local oxygen distributions, Fig. 7(b) presents three typical predictions of $N = 1$, 3, and 5. Generally speaking, as those presented in Fig. 7(a), the presence of the baffles leads to abrupt and high-peak variations of

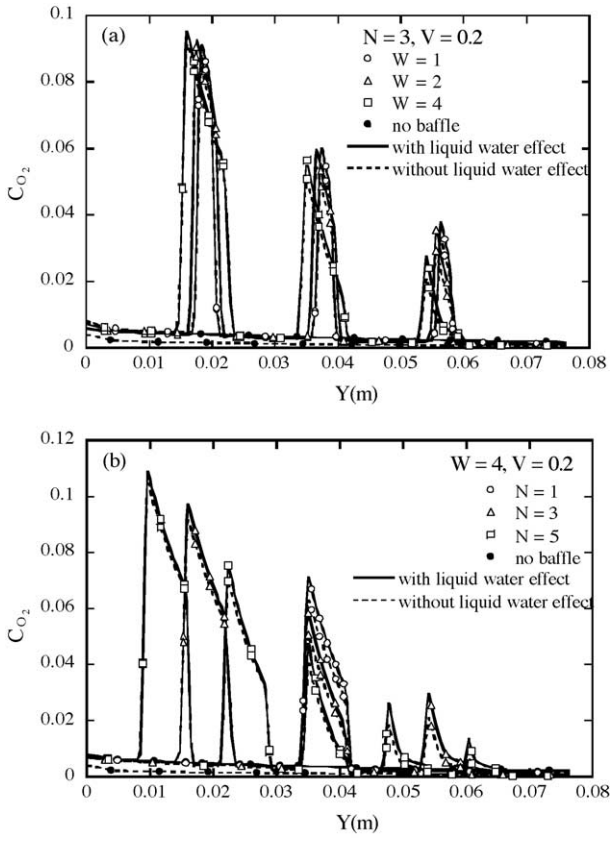

Fig. 7. Effects of baffle width and baffle numbers on the local distributions of oxygen mass fraction along the interface between the GDL and catalyst layer for $V = 0.2$ V.

the local oxygen mass fraction in the regions corresponding to the locations of the baffles. Comparing the local oxygen mass fraction in the region beneath the baffle, i.e., around the 1/2 channel length, in the three cases, it is shown that the local oxygen mass fraction reduces with increasing baffle number.

In analysis of the PEMFC, the airflow rate on the cathode side is one of the key operating parameters to the cell performance. To examine this effect, Fig. 8 shows the effects of air velocity on the cathode side on the performance curves of the PEMFC. In this work, the reactant inlet velocity of the values 0.44, 0.88 and 1.76 m s^{-1} are considered. The predictions in Fig. 8 disclose that a better cell performance is found for a case with a higher air velocity. The high velocity implies sufficient supply of the reactant gas, which reduces the mass transfer overpotential, delay the occurrence of the mass transport loss and then increases the limiting current density considerably. Besides, the model without consideration of liquid water effect over-predicts the simulated results of the *I–V* curves.

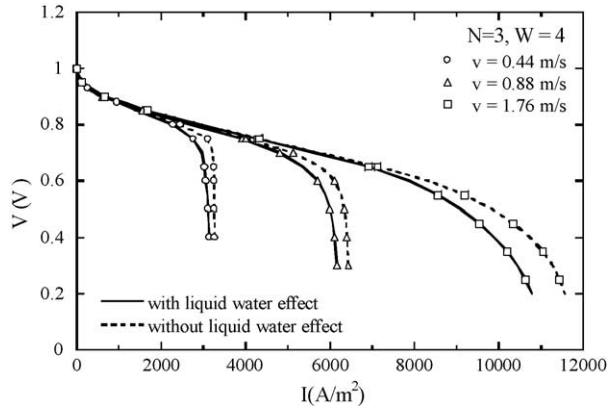

Fig. 8. Effects of air velocity on the cathode side on the cell performance.

5. Concluding remarks

With an appropriate design of the flow channel of the bipolar plate, the thermal and water management of the PEMFC can be achieved efficiently. To reach this end, a new concept of the flow channel design with baffles is proposed and analyzed in this work. To validate the concept, the detailed gas transport phenomena and cell performance with baffle effects in the flow channel are numerically investigated. What follows are the major findings.

1. Both the reactant transport and cell performance can be enhanced by the presence of the baffles in the flow channel of the bipolar plate, especially at the operating conditions of low voltage. The beneficial baffle effects become increasingly remarkable with increasing width and/or number of baffles in the tandem array.
2. Predictions demonstrate the baffle effects on the cell performance are dependent of operating conditions. At high operating voltages, the baffle effects enhance the gas fuel transport and raise the local current density in the upstream region but reduce them in the downstream part of the flow channel. The resultant influence of the presence of the baffles becomes insignificant due to offset of the two counter-effects. At low operating voltages, however, abrupt increases in local current density appear at the locations beneath the baffles. Although the values of the current density in the regions between the neighboring baffles reduce, noticeable enhancement in the resultant cell performance is still retained.
3. The predictions obtained by using the models with and without liquid water effects are of deviations, especially at the operating conditions of low voltage. Under this situation, the liquid water effect is significant and should be taken into account in the modeling.
4. With a higher air velocity on the cathode side, the local current density is increased and the cell performance can thus be enhanced. The high velocity of the reactant gas can reduce the mass transfer overpotential, delay the occurrence of the mass transport loss, and then increase the limiting current density considerably.

Acknowledgement

The study was supported by the National Science Council, the Republic of China through the grant numbers NSC 91-2218-E-211-001, NSC 91-2218-E-035-002, NSC 92-2623-7-002-006-ET, and 92-2212-E-035-027. In addition, the financial supports from ITRI and MOEA are also appreciated.

References

[1] T.E. Springer, T.A. Zawodizinski, S. Gottesfeld, Polymer electrolyte fuel cell model, J. Electrochem. Soc. 138 (1991) 2334–2342.
[2] J. Kim, S.M. Lee, S. Srinivasan, Modeling of proton exchange membrane fuel cell performance with an empirical equation, J. Electrochem. Soc. 142 (8) (1995) 2670–2674.
[3] D. Singh, D.M. Lu, N. Djilali, A two-dimensional analysis of mass transport in proton exchange membrane fuel cells, Int. J. Eng. Sci. 37 (1999) 431–452.
[4] N. Djilali, D. Lu, Influence of heat transfer on gas and water transport, Int. J. Therm. Sci. 41 (2002) 29–40.
[5] T.V. Nguyen, R.E. White, A water and heat management model for proton-exchange-membrane fuel cells, J. Electrochem. Soc. 140 (1993) 2178–2186.
[6] H.H. Voss, D.P. Wilkimson, P.G. Pickup, M.C. Johnson, V. Basura, Anode water removal: a water management and diagnostic technique for solid polymer fuel cells, Electrochim. Acta 40 (1995) 321–328.
[7] J.S. Yi, T.V. Nguyen, An along-the-channel model for proton exchange membrane fuel cells, J. Electrochem. Soc. 145 (4) (1998) 1149–1159.
[8] J.J. Baschuk, X. Li, Modeling of polymer electrolyte membrane fuel cells with variable degrees of water flooding, J. Power Sources 86 (2000) 181–196.
[9] T.V. Nguyen, A gas distributor design for proton exchange membrane fuel cells, J. Electrochem. Soc. 143 (5) (1996) L103–L105.
[10] D.L. Wood III, J.S. Yi, V. Nguyen, Effect of direct liquid water injection and interdigitated flow field on the performance of proton exchange membrane fuel cells, Electrochim. Acta 43 (24) (1998) 3795–3809.
[11] J.S. Yi, T.V. Nguyen, Multicomponent transport in porous electrodes of proton exchange membrane fuel cells using the interdigitated gas distributors, J. Electrochem. Sci. 146 (1999) 38–45.
[12] W. He, J.S. Yi, T.V. Nhuyen, Two-phase flow model of the cathode of PEM fuel cells using interdigitated flow fields, AIChE J. 46 (10) (2000) 2053–2064.
[13] S. Um, C.Y. Wang, Three-dimensional analysis of transport and reaction in proton exchange membrane fuel cells, in: Proceedings of the 2000 ASME International Mechanical Engineering Congress and Exposition, November 5–10, Walt Disney World Dolphin, Orlando, FL, 2000.
[14] S. Um, C.Y. Wang, K.S. Chen, Computational fluid dynamics modeling of proton exchange membrane fuel cells, J. Electrochem. Soc. 147 (2000) 4485–4493.
[15] A.S. Arico, P. Creti, V. Baglio, E. Modica, V. Antonucci, Influence of flow field design on performance of a direct methanol fuel cell, J. Power Sources 91 (2000) 202–209.
[16] W.-M. Yan, C.-Y. Soong, F. Chen, H.S. Chu, Effects of flow distributor geometry and diffusion layer porosity on reactant gas transport and performance of proton exchange membrane fuel cells, J. Power Sources 125 (2004) 27–39.
[17] W.-M. Yan, C.-Y. Soong, F. Chen, H.S. Chu, Transient behaviors of reactant gas transport and performance of PEM fuel cells, J. Power Sources, in press.
[18] S. Mazumder, J.V. Cole, Rigorous 3-D mathematical modeling of PEM fuel cells. II. Model predictions with liquid water transport, J. Electrochem. Soc. 150 (11) (2003) A1510–A1517.
[19] C.-Y. Soong, W.-M. Yan, C.Y. Tzeng, H.-C. Liu, F. Chen, H.S. Chu, Analysis of reactant gas transport in a PEM fuel cell with partially-blocked flow channel design, J. Power Sources, in press.
[20] C.Y. Chen, Effect of interdigitated flow channel design on the performance of proton exchange membrane fuel cells, Master Thesis, Department of Mechatronic Engineering, Huafan University, Taipei, Taiwan, 2003.